Smart Mater. Struct. **20** (2011) 094014 (13pp) doi:10.1088/0964-1726/20/9/094014

Bioinspiration from fish for smart material design and function

G V Lauder[1], P G A Madden[1], J L Tangorra[2], E Anderson[3] and T V Baker[3]

[1] The Museum of Comparative Zoology, Harvard University, 26 Oxford Street, Cambridge, MA 02138, USA
[2] Department of Mechanical Engineering, Drexel University, Philadelphia, PA 19104, USA
[3] Department of Mechanical Engineering, Grove City College, Grove City, PA, USA

E-mail: glauder@oeb.harvard.edu

Received 31 January 2011, in final form 13 April 2011
Published 30 August 2011
Online at stacks.iop.org/SMS/20/094014

Abstract
Fish are a potentially rich source of inspiration for the design of smart materials. Fish exemplify the use of flexible materials to generate forces during locomotion, and a hallmark of fish functional design is the use of body and fin deformation to power propulsion and maneuvering. As a result of nearly 500 million years of evolutionary experimentation, fish design has a number of interesting features of note to materials engineers. In this paper we first provide a brief general overview of some key features of the mechanical design of fish, and then focus on two key properties of fish: the bilaminar mechanical design of bony fish fin rays that allows active muscular control of curvature, and the role of body flexibility in propulsion. After describing the anatomy of bony fish fin rays, we provide new data on their mechanical properties. Three-point bending tests and measurement of force inputs to and outputs from the fin rays show that these fin rays are effective displacement transducers. Fin rays in different regions of the fin differ considerably in their material properties, and in the curvature produced by displacement of one of the two fin ray halves. The mean modulus for the proximal (basal) region of the fin rays was 1.34 GPa, but this varied from 0.24 to 3.7 GPa for different fin rays. The distal fin region was less stiff, and moduli for the different fin rays measured varied from 0.11 to 0.67 GPa. These data are similar to those for human tendons (modulus around 0.5 GPa). Analysis of propulsion using flexible foils controlled using a robotic flapping device allows investigation of the effect of altering flexural stiffness on swimming speed. Flexible foils with the leading edge moved in a heave show a distinct peak in propulsive performance, while the addition of pitch input produces a broad plateau where the swimming speed is relatively unaffected by the flexural stiffness. Our understanding of the material design of fish and the control of tissue stiffness is still in its infancy, and the development of smart materials to assist in investigating the active control of stiffness and in the construction of robotic fish-like devices is a key challenge for the near future.

(Some figures in this article are in colour only in the electronic version)

1. Introduction

Fish, as a result of their 500 million year evolutionary history, have evolved a remarkable variety of materials and configurations of these materials that allow them to swim, feed, reproduce, and locomote in the aquatic realm. Fish represent an elegant solution to the problem of moving through water at larger length scales. And although other types of evolutionary design solutions to this problem have occurred during the history of life, fishes are well known for the diversity of their locomotor abilities, with some species able to achieve high-speed locomotion and migrate many thousands of miles, while other species excel at low-speed maneuverability. Fishes are also striking for the diversity of body shapes and fin positions and sizes (Helfman *et al* 1997, Lauder 2006, Marshall 1971), with noteworthy examples including the variety of tail shapes

which range from the asymmetrical shape of the shark tail to wing-like tuna tails, and the highly flexible elongate tails of many smaller maneuvering species. A similar diversity exists in the placement of fins around the body axis and in the size and shape of these fins (Young 1981, Webb 1975).

Another key characteristic of fish propulsion systems is the use of flexible materials or combinations of materials. Most man-made systems designed for aquatic propulsion are composed of rigid materials, while fish execute their locomotor behaviors by activating flexible bodies and fins. However, despite some recent significant advances in understanding the material composition and function of fish (reviewed in Summers and Long 2006); also see the overview of fish biomechanics in Shadwick and Lauder (2006), there is still only the most general understanding of the materials that make up a fish body and fins and how these materials function during natural behaviors such as swimming. For example, the mechanical design of fin rays that support the fins of fishes are very poorly understood, and yet these elements are critical to understanding how fish swim because they determine fin conformation and allow muscular activation of fin motion (Lauder and Madden 2007, Lauder *et al* 2007).

One of the current impediments to building our knowledge about fish material design is that we lack good model systems for laboratory investigation of individual mechanical properties of fish structures. As a result, even basic biomechanical issues such as how body stiffness affects locomotor performance and swimming speed are not well understood. If we are to take inspiration from fish and use fish as a platform for constructing flexible materials that can be used in robotic devices or for new types of mechanical designs, then we need to have a better understanding of how fish are constructed, of the material properties of the components, and to develop test platforms that allow us to answer basic biomechanical questions about how fish function in the aquatic environment.

In this paper, we first provide a brief overview of some key aspects of fish mechanical design, and then focus on two areas that are key to making progress in understanding fish biomechanics, with specific implications for fish-inspired smart material construction: the mechanics of fish fin rays, and the function of simple undulatory fish swimming models varying in flexural stiffness. The underlying theme of the paper is that a great deal more information is needed about the design and function of flexible materials that make up the fins and body of fishes.

2. Brief overview of fish functional design

Fish vary greatly in basic design, but almost all species of the loosely defined group termed ‘fishes’ (primarily sharks and relatives, and bony or ray-finned fishes) possess a central backbone that is stiff relative to the surrounding soft tissues (figures 1(A) and (B)). Attached in various ways to this backbone are the fins, and the presence of multiple propulsive fins that are used to produce fluid forces is a hallmark of fish functional design. In most fish, the body is surrounded by fins, and the caudal (tail fin), anal and dorsal fins, and pectoral and pelvic fins (all under active muscular control) allow fish to position their body accurately in the three-dimensional fluid environment, and to generate and control fluid forces.

The fins of bony fishes consist of a fan-like membrane supported by fin rays (figures 1(C)–(E)). Fin rays may develop into solid spines (figure 1(C)) or remain separate throughout most of their length, and the fin rays of most fishes are segmented (figures 1(E) and 2). The fin rays of bony fishes have a remarkable bilaminar structure that has been described generally in several recent analyses (Alben *et al* 2007, Lauder 2006, Lauder *et al* 2006), but much remains to be learned about the mechanical properties of fin rays in bony fishes (figure 2). Briefly, fin rays are composed of two halves (termed hemitrichs, figure 2(A)) that can slide past each other, allowing the fin ray to curve along its length as a result of differential muscle activation at the base (Alben *et al* 2007, Lauder 2006). The ability to actively curve the propulsive surface of fins is a hallmark of bony fishes, and distinguishes the propulsive mechanics of these appendages from similar propulsors such as bird feathers and insect wings. Sharks and rays have fins with fin rays, but these rays are solid and do not have the two hemitrich structure that allows active control of curvature. Each of these two halves is composed of small bony segments that are attached to each other (figures 1(E) and 2(B)). Fin rays can branch toward the distal end (away from the base) and in this case each of the hemitrichs branches to maintain the bilaminar structure from base to the tip. The region of the fin ray near the base is often unsegmented. Each of the two hemitrichs often has a concave structure with small blood vessels and nerves that run out along the length of the ray (figure 2(B)). Fin ray structure is also discussed in Goodrich (1904), Geraudie and Meunier (1982), Geraudie (1988), Haas (1962), Lanzing (1976), and papers by Geerlink and Videler (1987), Geerlink (1989).

Fin rays attach to the body (figure 3) via a series of small bony elements (radials) that allow the fin rays to rotate around their base as a result of the activation of fin muscles. Each hemitrich also has a complex expanded head at the base that serves as the site of attachment of up to four separate muscles that permit active control over fin motion, and allow the fin to expand and contract like a fan thus changing surface area, and to produce limited rotation and twisting (figure 3). Fin muscles provide the differential force at the base of the two hemitrichs that cause the whole fin ray to curve as shown in figure 2(C) (Lauder 2006, Lauder and Madden 2006).

The body of fishes consists of a flexible backbone surrounded by segmented muscular tissue with a complex topology, the functional significance of which is not yet fully understood (Brainerd and Azizi 2005, Jayne and Lauder 1994, 1995a, Alexander 1969) (figure 1(A)). The body muscles of bony fishes are patterned into a series of W-shaped segments termed myomeres which are activated sequentially by the nervous system to produce an undulatory wave of bending that passes down the body, and this wave of muscular activity causes the segmented backbone to bend in a wave-like pattern (Lauder and Tytell 2006, Jayne and Lauder

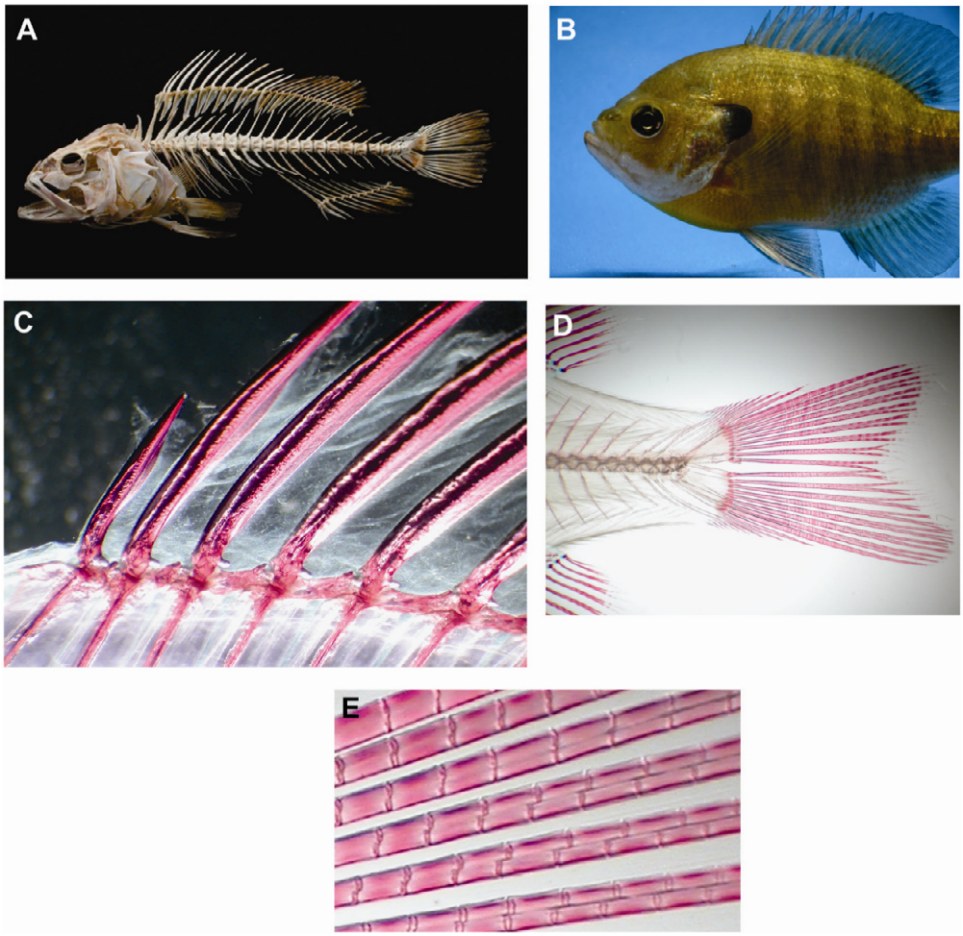

Figure 1. Overview of fish anatomy. (A) Skeleton of a perch-like bony fish showing the segmented vertebral column and the major median fins. (B) Image of a bluegill sunfish, *Lepomis macrochirus*, to show the dorsal fin (with both a spiny anterior and posterior fin region with flexible fin rays), the pectoral, pelvic, and anal fins. (C) Spiny portion of the dorsal fin in a bluegill sunfish. (D) Caudal (tail) region of a bluegill sunfish. (E) Close-in view of fin rays to show that each ray is composed of jointed bony segments; a thin fin membrane is present between each fin ray. Red color indicates alizarin stain for bone.

1996). A considerable number of studies have been conducted on fish muscular properties, and work-loop analyses have demonstrated how these properties change along the body and how power is generated by longitudinal fish musculature (Syme 2006, Johnston and Salamonski 1984, Johnston 1981, Rome *et al* 1992). Wave-like deformations of the fish body with increasing amplitude from head to tail result in the production of thrust which is manifested in the water as a series of vortices shed into the wake by the bending body (Webb 1975, Lauder and Tytell 2006).

Although some important studies have provided data on the mechanics of fish backbones (Long 1992, Long *et al* 1996, Long and Nipper 1996, Hebrank 1982, Porter *et al* 2006), the role of body musculature in modulating stiffness during swimming and the mechanisms by which fish can alter flexural stiffness are as yet poorly understood. Even basic features of undulatory locomotion such as the extent to which changing flexural stiffness of the body can affect propulsion are not well characterized (McHenry *et al* 1995), and we have only a general idea of how or if fish tissue stiffness is actively controlled to modulate locomotor performance.

3. Mechanics of fish fin rays

In order to investigate the mechanical properties of bony fish fin rays, we performed experiments on fresh rays from bluegill sunfish (*Lepomis macrochirus*) under a variety of conditions (figure 4). Individual fin rays were removed from fins and each hemitrich clamped separately in small clips attached to micrometer actuators allowing independent displacement of each hemitrich as well as measurement of the force exerted to displace one hemitrich relative to the other (figure 4(A)). This arrangement also allowed us to quantify fin ray curvature relative to hemitrich displacement (figure 4(B)). Cantilever measurements of the force output at varying sites along the fin ray relative to force and displacement inputs at the hemitrichs (figure 4(C)), and three-point bending tests (figure 4(D)) to calculate the fin ray Young's modulus were also performed. Micro-CT scans of fin rays allowed calculation of the second moment of area along each fin ray. All results reported here are for bluegill sunfish pectoral fin rays.

Displacing one hemitrich relative to the other generates curvature along the length of the fin rays, and the shape

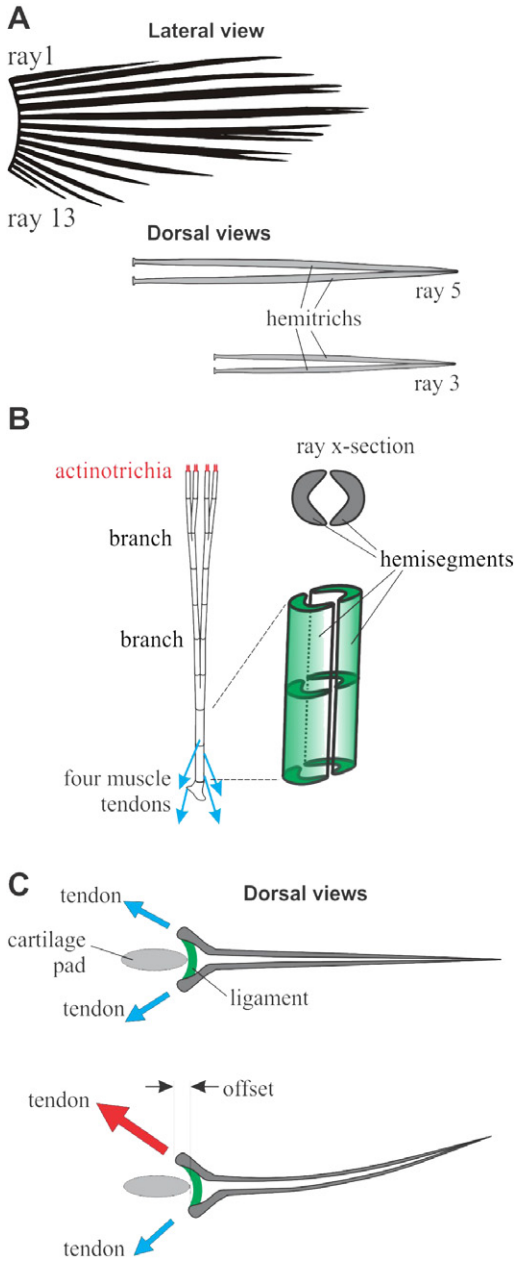

Figure 2. Schematic diagrams of ray anatomy in ray-finned fishes. (A) Lateral and dorsal views of a whole pectoral fin and two fin rays, respectively. The two hemitrichs that make up each fin ray can be seen in the dorsal view of individual fin rays. (B) Schematic diagram of the structure of an individual fin ray. Each ray has two halves called hemitrichs that are semilunate (shown in the ray cross-section). Each hemitrich is composed of multiple bony hemisegments. Each ray can branch one or more times along its length. The tips of the hemitrichs are joined by fibrous actinotrichia. (C) Simplified fin ray bending mechanism. Forces are applied to hemitrichs via muscles attaching through tendons near the hemitrich base. When the applied forces move one hemitrich relative to the other (large red arrow) to create an offset (labeled in figure) the fin ray bends. A ligament (green) that joins the bases of the hemitrichs slides over a supporting cartilage pad. Portions of this figure modified from Alben *et al* (2007).

of the ray varies depending on its location within the fin (figure 5). In general, the distal and basal thirds of fin rays show relatively little curvature, while the greatest curvature occurs in the middle region of the fin (figure 5). The maximum curvatures of each fin ray produced by hemitrich displacement are approximately linear functions of the offset of the bases (figures 6(A) and (B)). Fin rays differ considerably in the extent of curvature for a given hemitrich base offset. Rays in the middle of the fin give curvature values of around 0.3 mm^{-1} for a 0.2 mm displacement, and the tips of the fin rays displace 5–10 mm from the centerline for an 0.2 mm offset. These curvature values are similar to those observed in kinematic studies of the fins of swimming fishes (Standen and Lauder 2005, 2007, Taft *et al* 2008), and indicate that these *in vitro* manipulations of fin rays produce natural deformations. Measurement of the force required to displace hemitrichs relative to each other show that fin rays at different locations within the fin differ considerably from each other in the extent of force needed to produce a given curvature or tip displacement (figures 6(C) and (D)): a force of 30 mN applied to one hemitrich of the pair can generate between 0.1 mm^{-1} and 0.4 mm^{-1} curvature and 3.5 mm and 8.5 mm tip displacement respectively depending on the fin ray.

Cantilever force measurements to quantify the relationship between hemitrich offsets and force inputs at the hemitrich bases and output at the fin ray (method shown in figure 4(C)) show that the first two fin rays (joined together tightly and thus treated as a unit) produce much more force out for a given offset input than the other fin rays (figure 7). A 0.15 mm offset generates almost 20 mN force near the end of the fin ray for ray 1 + 2, but only 1–4 mN force for other fin rays (figure 7(A)). Simultaneous measurements of force input and output show that the fin ray design is not particularly effective at transmitting force, as a 50 mN force input only produces 1.5 mN of force near the tip of the ray (figure 7(B)).

Three-point bending tests on bluegill sunfish fin rays show that there is considerable variation between locations along the fin rays (figure 8) and that the basal region of each ray is much stiffer than the distal (outer) region (figure 8(A)). Fin rays within the fin differ considerably in their force–displacement curve with smaller rays on the ventral margin of the fin (rays 11 and 12) being much less stiff than other rays in the fin.

Because fin rays are reported to possess a series of connections along the lengths of the two hemitrichs, and mathematical models of fin ray function indicate the importance of these connections compared to the attachment at the tips (Alben *et al* 2007) we made a series of measurements of tip displacement versus force input for fin rays in which we sequentially cut the ray shorter from the tip toward the base (figure 9). In figure 9(B), each curve ii, iii, and iv compares intact fin ray displacements at the point of the same-colored dot in figure 9(A) (online figure version is in color), with displacements after cutting the fin ray. These data show that cutting the fin ray to remove any tip connections and to progressively make the ray shorter does not alter the displacement–force plot slope as compared to an intact fin ray: both the dashed lines and solid lines in figure 9(B) are very similar for each fin ray length compared to the same position in the intact ray. Shorter sections of fin rays thus show the same response to a given force input as the intact ray, indicating clearly that the two hemitrichs possess a

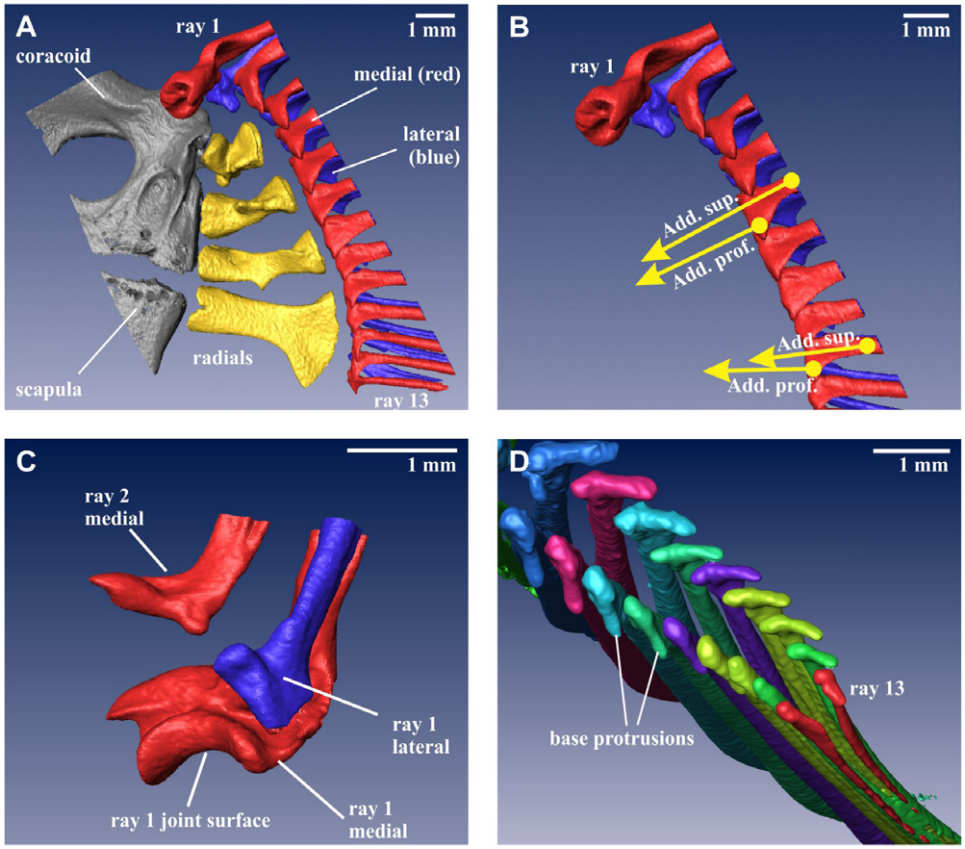

Figure 3. Three-dimensional reconstructions from micro-CT scans of fin rays and the supporting skeleton in a bluegill sunfish, with the major elements segmented and indicated in different colors. (A) The pectoral girdle with the scapula, coracoid, and radials support the pectoral fin rays. Medial hemitrichs are shown in red and lateral hemitrichs are shown in blue. (B) Most hemitrichs have two tendon attachment points. The adductor superficialis and adductor profundus pectoral fin muscles attach to the medial hemitrichs (yellow arrows). The abductor profundus and abductor superficialis attach to the lateral hemitrichs (not shown). (C) The medial hemitrich of the first ray has a large base structure that articulates with the coracoid. The lateral hemitrich base is much smaller. Unlike other rays, the hemitrichs of ray 1 are fused over much of their lengths, and the bases of the two hemitrichs are asymmetrical in structure. The base of the ray 2 medial hemitrich is shown for comparison. (D) Protrusions at the base of the hemitrichs are attachment points for muscle tendons. The ventralmost nine fin rays are each shown in a different color, and in an oblique view down the fin from proximal to distal.

series of interconnections along their length that dominate the mechanical behavior of the system. It is currently unclear just what the nature of the connection between the two hemitrichs of fish fin rays is, and what the material located inside the two semilunar hemitrichs consists of. Certainly small blood vessels, lymphatics, and nerves may be present, but these structures will not bridge the two hemitrichs. There has been some suggestion of elastic fibers connecting the two hemitrichs of a fin ray (Videler 1993, Geerlink and Videler 1987), but considerable future work will be needed to convincingly identify the specific components that are responsible for the behavior of the bilaminar fin ray design.

Data from the three-point bending tests along with micro-CT scans of bluegill sunfish fin rays were used to estimate the second moment of area of individual fin rays and also the modulus of elasticity (Young's modulus). Table 1 shows a summary of these data and calculated values of the modulus of elasticity of different fin rays. The mean modulus for the proximal (basal) region of the fin rays was 1.34 GPa, but this varied from 0.24 to 3.7 for different fin rays. The distal fin region was less stiff, and moduli for the different fin rays measured varied from 0.11 to 0.67 GPa. These data are similar to that of human tendon (modulus around 0.5 GPa), which is not too surprising given that adjacent fin ray segments are connected by collagenous fibers, and that bending of fin rays would stretch these fibers. Hence, fin ray stiffness may be dominated by the same collagenous proteins found in tendons.

4. Flexible foils as models of fish propulsion

Understanding fin ray mechanics is a critical part of learning about the material design of fishes, but a second key feature of fish design is the flexible body that is used in a wave-like undulatory fashion to power propulsion in fishes. Body deformations have frequently been quantified to calculate wave velocities, the amplitude of side-to-side excursions down the body, and locomotor efficiency (e.g. Webb 1975, 1978, Webb and Keyes 1982, Lauder and Tytell 2006). Measurements of body wave characteristics have given rise to the common terminology used to characterize different modes of undulatory locomotion in fishes, such as the anguilliform (or eel-like) pattern of body waves compared to a trout-like

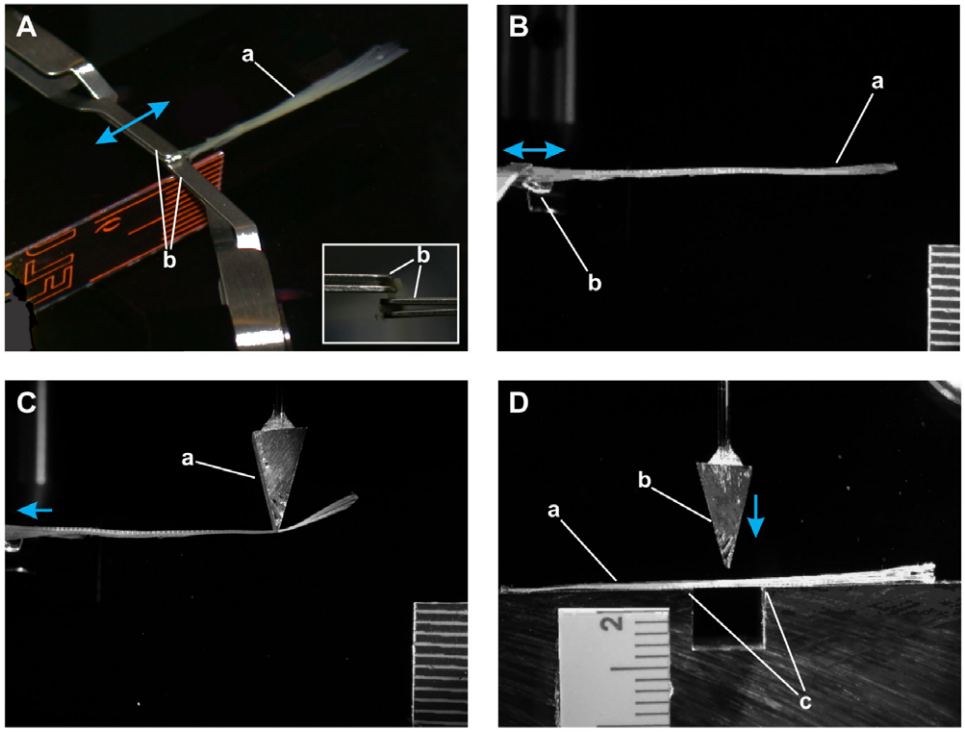

Figure 4. Experimental methods. (A) Oblique view of hemitrich clips holding a fin ray. The fin ray (a) is submerged in water and two clips (b) hold the two hemitrich bases. To bend the rays, the upper clip is shifted parallel to the ray direction (blue arrow). Inset: view from the base end of the fin ray. Each hemitrich base is held by a single clip. (B) Curvature measurements. The fin ray (a) is held horizontally as the hemitrich offset and force are changed at the base (b). Curvature and vertical tip displacement are measured from digital photographs. (C) Cantilever force measurements. The vertical force at the distal end of the ray is measured with a probe (a) as the hemitrich offset and force are changed. (D) Three-point bending measurements. A ray (a) is deflected by a probe (b) which is lowered between two supporting points (c). Stiffness of the ray is measured by holding one or both hemitrichs fixed and measuring force as the probe is moved vertically. Scales shown are marked at 1 mm intervals. Portions of this figure modified from Alben *et al* (2007).

Table 1. Area moments, flexural stiffness and Young's modulus of bluegill sunfish fin rays.

Ray	Proximal three-point stiffness[a] (mN mm^{-1})	Distal three-point stiffness[a] (mN mm^{-1})	Proximal summed moments[b] ($\times 10^{-3}$ mm^4)	Distal summed moments[b] ($\times 10^{-3}$ mm^4)	Proximal modulus (GPa)	Distal modulus (GPa)
1	73 ± 5.5		0.10 ± 0.07		3.7	
2	270 ± 40	34 ± 20	0.93 ± 0.22	0.27 ± 0.07	1.5	0.67
5/6	330 ± 240	26 ± 9.5	4.02 ± 1.04	0.43 ± 0.29	0.66	0.11
8	140 ± 15	23 ± 20	1.29 ± 0.70	0.34 ± 0.15	0.58	0.36
11/12	12 ± 5.6		0.26 ± 0.19		0.24	
Mean mod. (range)					1.34 (0.24–3.72)	0.38 (0.11–0.67)

[a] Three-point bending stiffness: values are mean ± 2 standard errors.

[b] Proximal summed moments: only one moment (and hence modulus) could be measured on rays 1, 11, and 12 due to their short lengths.

(carangiform mode) or tuna-like swimming (thunniform wave characteristics). Much of this terminology has been developed from inaccurate measurements of fish midline deformation (Lauder 2006), but it persists in the literature as a shorthand way of describing the pattern of body deformation used during swimming by fishes of differing body shape.

To date the vast majority of such studies of fish swimming have been necessarily descriptive because of our inability to manipulate a freely swimming fish and alter specific features of the body that might influence swimming performance. For example, ideally we would like to be able to change the length of a fish, its aspect ratio, and body flexural stiffness to determine how each of these factors in isolation influences swimming speed and waveform along the body.

In order to better control the myriad variables that could possibly affect the generation of undulatory waves along the body of swimming fishes, we have developed a computer-controlled robotic flapping foil device that allows us to measure the effect of different flexible foil motion programs and materials on swimming speed. This device and details of self-propelled swimming speed measurement are described in Lauder *et al* (2007). Foils of different flexible materials are

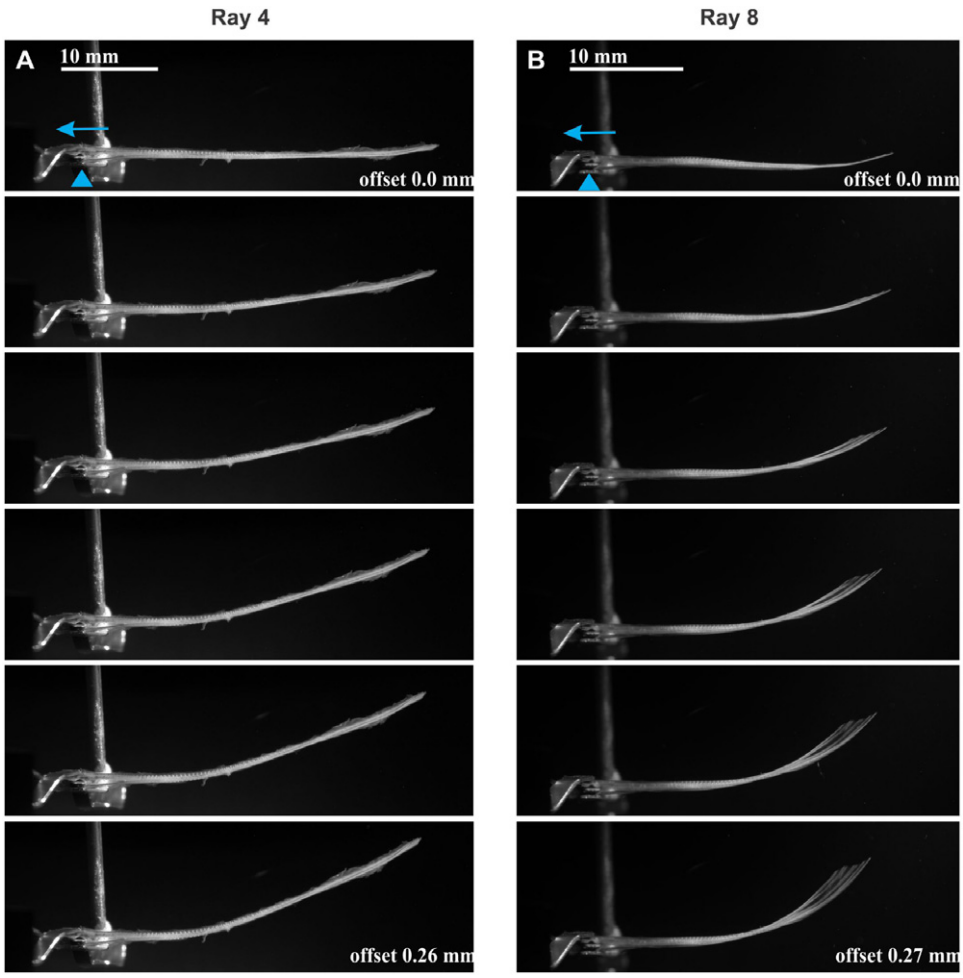

Figure 5. Image sequence of rays as hemitrich offset is increased. The upper hemitrich is being moved to the left (blue arrows in top images) while the lower hemitrich is held fixed (blue triangles). (A) Ray 4: hemitrich offset changes from 0 to 0.26 mm in steps of approximately 52 μm. (B) Ray 8: hemitrich offset changes from 0 to 0.27 mm in steps of approximately 55 μm. Ray 4, length = 40 mm. Ray 8, length = 29 mm. Note the differences in the location of maximum curvature between these two fin rays.

set in motion and the flow speed in the recirculating flow tank is tuned (using a LabView program) to match foil swimming speed. This Labview program that takes input from linear encoders on the flapping foil robotic apparatus to tune the flow tank speed so that the mean position is constant over a flapping cycle. Our force measurements from an ATI six-axis force/torque sensor on the foil shaft confirm that when the foil is self-propelling, the thrust force oscillations integrated over a flapping cycle equal zero. This proves that we have accurately tuned the flow speed to a mean exact self-propelled speed. In this way, foils swim at their natural speed, the point at which thrust and drag forces balance each other when averaged over each flapping cycle, and measuring this speed provides an indication of propulsive effectiveness. In this paper we present data on the effect of altering flexural stiffness on swimming performance, measured as self-propelled swimming speed. Figure 10 shows the flapping foil apparatus and panels A and B show how foils are attached to a rigid stainless steel sting (holding rod) that can be programmed to move in both heave (side-to-side) and pitch (rotating around the long axis). Foil propulsion occurs as the result of the interaction between the stiffness of the foil material itself, and the fluid forces on the foil. This structure–fluid interaction is critical to propulsion and determines the characteristics of the propulsive waveform.

Testing foil propulsion in still water provides an entirely misleading picture of swimming performance as can be seen in figure 10 panels (C) and (D) where the waveform produced by a flexible foil (flexural stiffness of this foil = 3×10^{-6} N m^2) is compared for motion in still water and when swimming at the self-propelled speed. In still water, the foil produces a complex and chaotic waveform when heave motion is imparted to the leading edge, and there is no regularity to the waves that move down the length of the foil (figure 10(C)). When the foil is allowed to self-propel at its natural swimming speed (figure 10(D)), it assumes a distinct sinusoidal shape that results from the fluid–structure interaction. Thus, quantifying the effect of flexibility on propulsion requires self-propelled conditions, and the lower the flexural stiffness, the greater the effect that the fluid motion has on swimming shape.

Figure 11 shows the results of experiments in which the propulsion of foils of different flexural stiffness was measured under conditions of heave actuation only, and then with pitch motion added to the heave. When flexible foils are moved in

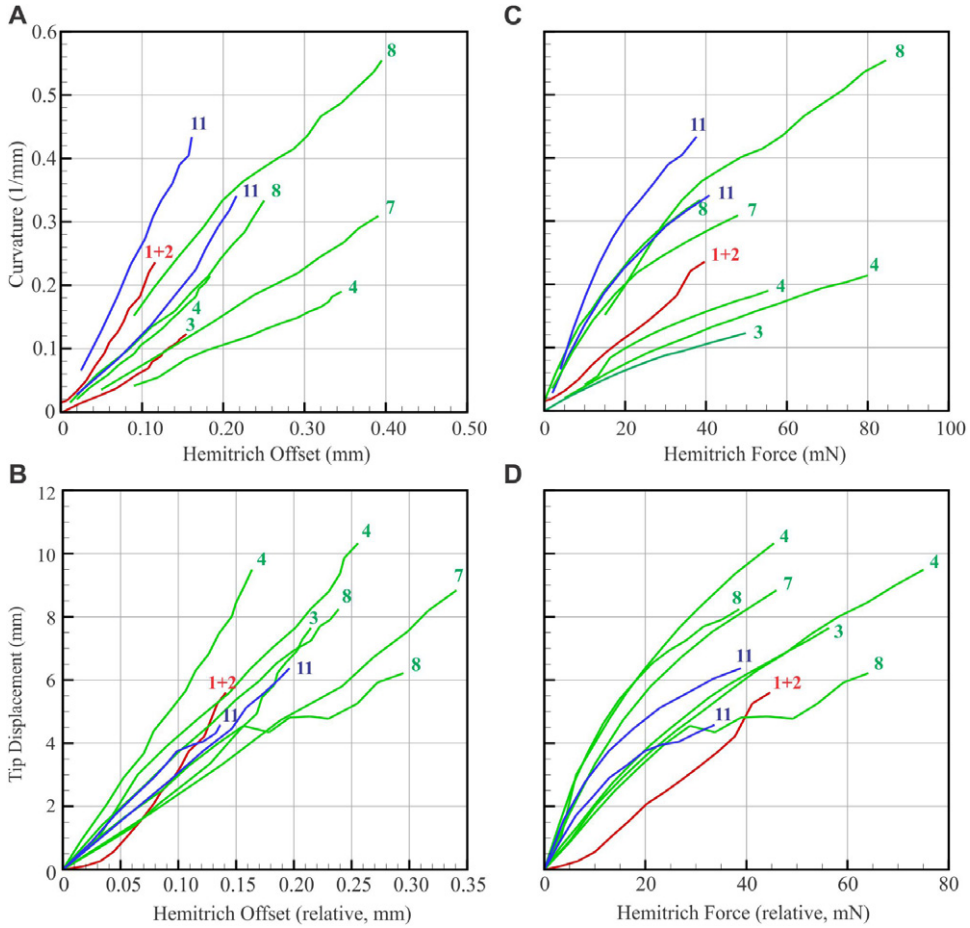

Figure 6. Curvature and vertical tip displacement of the fin ray versus hemitrich offset and hemitrich force. One hemitrich is held fixed while a force is applied to move the second hemitrich. (A) Average ray curvature versus hemitrich offset. (B) Vertical tip displacement versus hemitrich offset. (C) Average curvature versus hemitrich force. (D) Vertical tip displacement versus hemitrich force. Ray numbers associated with each curve are marked on the plot (1 + 2: rays 1 and 2 measured together). Red: dorsal rays. Green: middle rays. Blue: ventral rays. Plots are shown for nine rays from three different fish. There are between 9 and 16 measured points per curve. For clarity, markers for individual measurements are not shown.

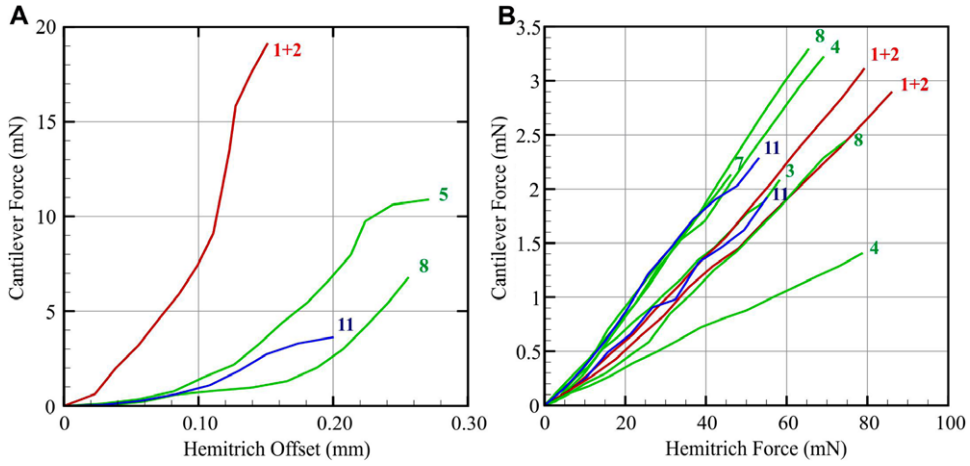

Figure 7. Cantilever force measurements. In panels (A) and (B), one hemitrich is held fixed while force is applied to move the second hemitrich. A probe near the distal end of the ray measures the force required to prevent the ray from curving upwards. (A) Cantilever force versus hemitrich offset for different fin rays. (B) Cantilever force versus hemitrich force. In panels (A) and (B), ray numbers for each curve are marked on the plot (1 + 2: rays 1 and 2 measured together). Red: dorsal rays. Green: middle rays. Blue: ventral rays. Panel (A) shows plots for four rays from a single fish. Panel (B) shows plots for 10 rays from three individuals. Plotted measurement curves have between 10 and 15 points.

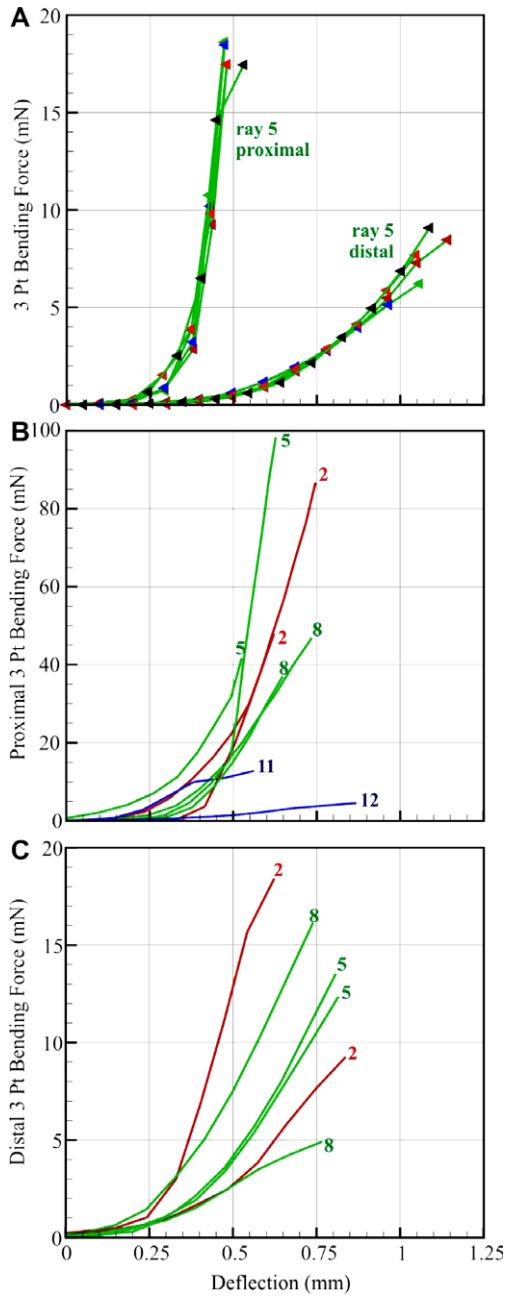

Figure 8. Three-point bending force versus fin ray deflection plots. (A) Five repeated trials on single ray (ray 5). Curves show repeated measurements at two points (one proximal and one distal) on the same ray. (B) Bending force in the proximal region for multiple rays. (C) Bending force in the distal region for multiple rays. Ray numbers for each curve are marked on the plot. Red: dorsal rays (ray 2). Green: middle rays (rays 5 and 8). Blue: ventral rays (rays 11 and 12). Panels B and C show plots for eight and six rays from two individuals. Where markers are not shown, plotted measurement curves have between 11 and 15 points.

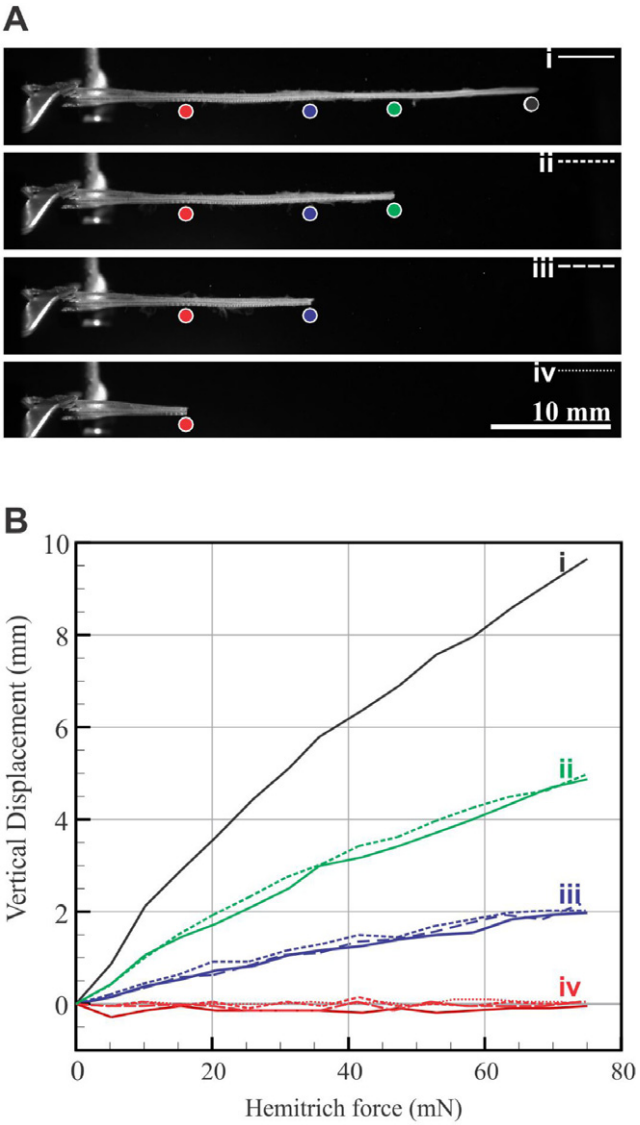

Figure 9. Effect of fin ray tip removal on mechanical properties. (A) Images of the intact ray (top image) and with increasing fractions of the ray removed. Symbol shapes represent positions along the ray. Symbol colors and the roman numerals correspond to the amount of the ray that has been removed (black (i): intact ray; green (ii), blue (iii), and red (iv): increasing portion of ray removed). (B) Vertical displacement versus hemitrich force for these rays of varying length. Symbol shape, symbol color, and roman numerals correspond to those used in the images in panel (A). So, curves (ii), (iii), and (iv) in panel (B) compare intact fin ray displacements at the point of the same-colored dot in panel (A) with displacements after cutting the fin ray. Plotted measurement curves each have 15 points. Removing portions of the fin ray does not change the relationship between vertical tip displacement and force input as indicated by the correspondence between the solid and dashed lines at each ray length.

heave only, there is a clear peak at which swimming speed is maximized. Foils that are either more or less flexible show reduced swimming performance. In contrast, adding a 20° pitch actuation to the leading edge of the foil in addition to the heave motion produces a broad plateau along which swimming performance does not change. Interestingly, maximum swimming speed is very similar for the two foil actuation modes, but there is no decline in performance as stiffness increases. These data show that swimming speed of flexible bodies in the water depends on the type and pattern of actuation, and on the value chosen for flexural stiffness.

There are certainly additional parameters that could influence self-propelled speed such as the phase relationship between heave and pitch, and changes in frequency and

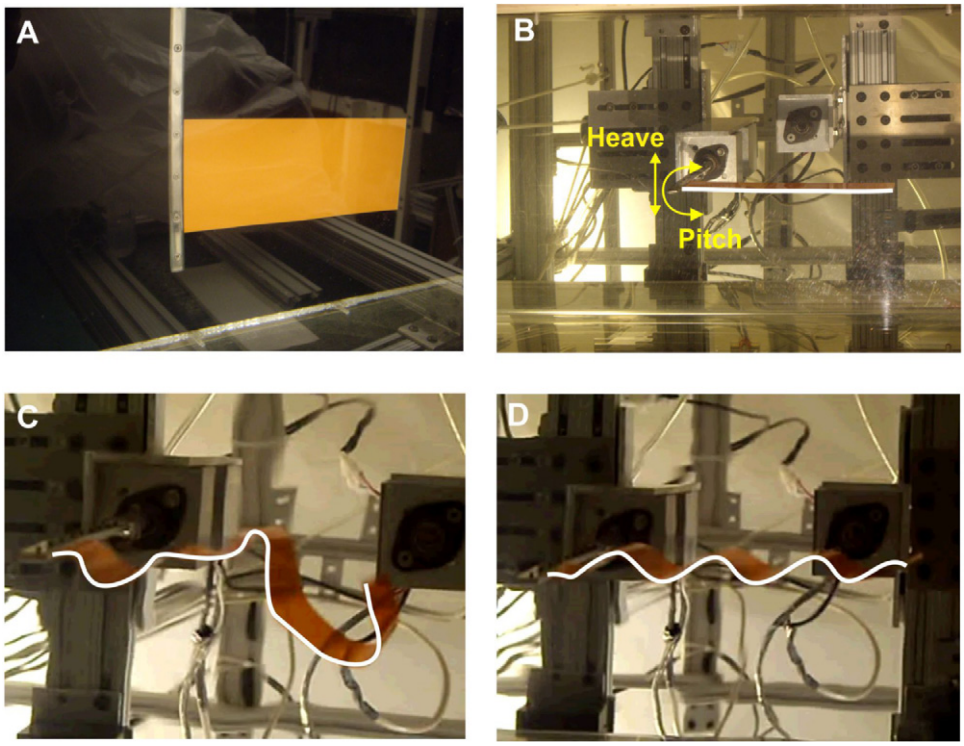

Figure 10. Experimental setup for testing flexible foil propulsion ((A) and (B)), and examples of a flexible foil swimming in still water (C) and at its self-propelled speed (D) of approximately 10 cm s^{-1}. The foil in panels (C) and (D) has a flexural stiffness of 3×10^{-6} N m^2. Foils are actuated in either heave, pitch, or both around the leading edge (B) and swim against an imposed flow in a recirculating flow tank where the flow speed has been tuned to match the swimming speed of the foil: foils are thus self-propelling. The effect of fluid motion on foil conformation can be seen by comparing the shapes of the foils in (C) and (D). White line shows the bottom edge of the foils in panels (B), (C), and (D), and actuation is of the foils in (C) and (D) is ± 1 cm heave; 2 Hz, no pitch.

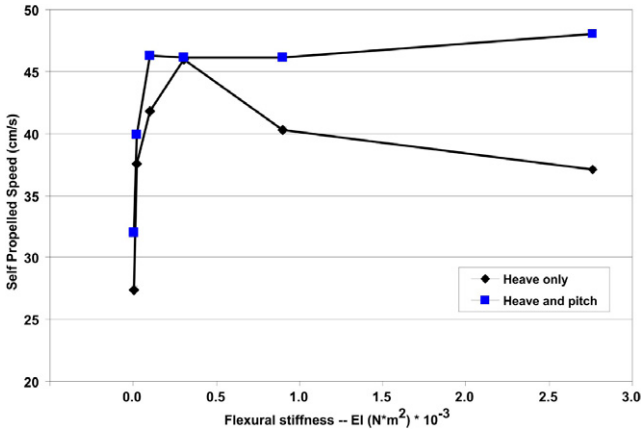

Figure 11. Self-propelled speed versus flexural stiffness for a set of flexible foils swimming in a recirculating flow tank. Each point represents a different foil. Values plotted are ± 1 standard error, but error bars are contained within the symbols and are not visible. Foils were 19 cm high, 6.8 cm long, and actuated at 1 Hz with ± 1.5 cm heave, or heave with $\pm 20°$ pitch motion added. Note the distinct peak for heave actuation, but the presence of a plateau for stiffer foils when pitch is added to the leading edge, even though maximum swimming speed does not change.

amplitude of the imposed leading edge motion. We have not presented results varying these parameters here, but such studies are needed in the future to understand more completely the full range of behaviors exhibited by swimming flexible foils.

The range of values represented in these experiments (figure 11) matches well with data on fish body flexural stiffness and these flexible foil experiments thus represent a reasonable model system for the study of fish propulsion using flexible surfaces. McHenry *et al* (1995) report values for flexural stiffness along the body of pumpkinseed sunfish *Lepomis gibbosus* that range from approximately 1×10^{-3} N m^2 near the head to 1×10^{-6} N m^2 near the tail. These values fall within the range of foil flexural stiffnesses plotted in figure 11, supporting the use of these flexible foils as models of fish locomotion. Long *et al* (2002) report flexural stiffness values of hagfish bodies in the range of 3×10^{-4} N m^2. This represents a point on the rising portion of the curves in figure 11 where the flexible foils self-propel at approximately 40–45 cm s^{-1}. A species of fish with a much greater flexural stiffness is the gar (genus *Lepisosteus*), which is in many ways a 'living fossil' covered with rows of large interlocking bony scales reminiscent of early ray-finned fishes of 300 million years ago (Lauder and Liem 1983). The scales contribute to a stiffer body with a flexural stiffness of about 0.06 N m^2 (Long *et al* 1996), about four to six orders of magnitude greater than the bodies of other fishes measured.

Changing the aspect ratio of self-propelling foils also has significant effects on locomotor performance. The diversity of fishes includes species with a wide range of caudal fin aspect

ratios, but it is not possible to isolate this trait independently of other differences among species in studies of live fishes to determine the effect of changes in aspect ratio alone on propulsive performance. Our experiments on flexible foil propulsion included studies of the effect of aspect ratio on swimming speed for materials with a given flexural stiffness, and we found that simply changing the orientation of a given rectangular foil shape from the long axis oriented horizontally (as in figure 10(A)) to a vertical orientation (while keeping all else constant, with actuation of ±1.5 cm heave, no pitch, at 1 Hz) more than doubled the self-propelled speed from 21.2 cm s^{-1} (±0.85 s.e.) to 46.0 cm s^{-1} (±0.24 s.e.) for material with a flexural stiffness of 0.3×10^{-3} N m^2. Moving propulsive mass closer to the axis of actuation thus greatly increases swimming speed, and allows flexible materials to impart more of the imposed actuation movement into the water as thrust. A more flexible material with a higher aspect ratio can swim with the same speed as a stiffer material formed into a lower aspect ratio foil.

5. Learning from fish: needs and prospects for smart materials

Fish provide a multitude of potential models for smart material design, including fin rays, fin webbing, a flexible body, jointed backbone, and segmental musculature. The development of smart materials that represent one or more aspects of these features would be of tremendous use. Researchers interested in testing hypotheses of the function of fish anatomical features could use smart materials to develop models for undulatory propulsion. More specifically, the simple flexible foil robotic models discussed above are passive representations of fish swimming. Traveling waves of a generally similar character to those produced by fish are generated by actuation at the leading edge of the foil, but swimming fishes have segmental muscles down the body that provide power input along the length of the fish. The development of controllable active materials that could be incorporated into the design of fish models would be a significant advance and allow biomechanists to test models of fish propulsion in ways not currently possible. For example, the successful incorporation of contractile polymers or IPMCs (ionic polymer metal composites) into a flexible foil would allow active elements to contribute to generating undulatory patterns along the body, and some designs using this approach have been suggested in the literature (Kim and Tadokoro 2007). In addition, contractile polymers, FMCs (flexible matrix composites) and IPMCs have begun to appear in early designs of fins and propulsive surfaces (Tangorra *et al* 2007a, Chen *et al* 2010, Yim *et al* 2007, Zhang *et al* 2010, Shan *et al* 2006, Yeom and Oh 2009, Chen and Tan 2010), as well as in actuated control flaps (Madden *et al* 2004a, 2004b) on airfoil-like designs. And, actuators made from peizoelectric composites (Wiguna *et al* 2009), shape memory alloys (Shinjo and Swain 2004, Wang *et al* 2008), muscle-tissue materials (Feinberg *et al* 2007), and electromechanical systems (Curet *et al* 2011a, 2011b), could all be brought to bear on the problem of designing fish-like actuators and devices. Being able to adjust the stiffness of design components would allow the effect of dynamic changes in stiffness on locomotor performance to be assessed (Mutlu and Alici 2010). The promise of this new smart material technology is great, as it would introduce an active contractile element into studies that have until now emphasized the passive properties of flexible foil propulsion. And the availability of such controllable elements would allow a wide range of experimental tests of propulsion such as altering the phasing of activation of contractile elements along the flexible surface, a topic of considerable interest to researchers in fish locomotion (Shadwick *et al* 1999, Donley and Shadwick 2003, Rome *et al* 1984, Jayne and Lauder 1995b), but a topic on which experimental study has not yet been possible due to the constraints of working on live fish.

Not only can the development of new controllable smart materials allow biologists and biomechanists to test hypotheses about aquatic propulsive systems in ways not previously possible, but smart material design and fish biology can also achieve a profitable interaction in the development of new types of robotic models for aquatic propulsion with controllable and deformable surfaces (Tangorra *et al* 2007a). At present, most robotic fish models of whole fish or fish fins use a single rigid or uniformly flexible membrane to transmit force to the water (Kato 1999, 2000), and even in the more complex robotic fish models with jointed and individually actuated fin rays (Tangorra *et al* 2010, 2007b) the surface conformation of the propulsor cannot be easily altered. The advent of smart materials that allow surface conformational changes in a controlled way will greatly enhance our ability to design robotic fish-like devices with performance that is closer to real animals.

Two overarching themes that emerge from biomechanical studies of fish propulsion are (1) that locomotion involves the use of flexible materials, and (2) that fish have the ability to actively control the stiffness of their flexible propulsive surfaces during swimming and appear to use this ability to tune locomotor dynamics (Flammang 2010, Tangorra *et al* 2010, Long *et al* 2006, 2002, Lauder and Madden 2007, Alben *et al* 2007). And the extent to which body and fin stiffness changes moment-to-moment during locomotion in a time-dependent fashion has not yet been addressed. Many questions remain about how stiffness tuning, if present, is achieved, and to what extent fish can modulate stiffness of the body and fins to optimize propulsive performance. The advent of smart materials that can be used to assist in answering these questions would be a great benefit for biologists, roboticists, and materials engineers interesting in understanding the mechanical basis for the diversity of fish locomotor patterns seen in nature.

Acknowledgments

This work was supported ONR grant number N00014-09-1-0352 on fin neuromechanics monitored by Dr Thomas McKenna, an ONR-MURI Grant N00014-03-1-0897 on fish pectoral fin function monitored by Dr Thomas McKenna and

initiated by Dr Promode Bandyopadhyay, and by NSF EFRI-0938043. We thank members of the Lauder and Tangorra Labs for many helpful discussions on fish fins and flexible flapping foil propulsion.

References

Alben S, Madden P G A and Lauder G V 2007 The mechanics of active fin-shape control in ray-finned fishes *J. R. Soc. Interface* **4** 243–56

Alexander R M 1969 The orientation of muscle fibers in the myomeres of fishes *J. Mar. Biol. Assoc. UK* **49** 263–90

Brainerd E L and Azizi E 2005 Muscle fiber angle, segment bulging and architectural gear ratio in segmented musculature *J. Exp. Biol.* **208** 3249–61

Chen Z, Shatara S and Tan X 2010 Modeling of biomimetic robotic fish propelled by an ionic polymer–metal composite caudal fin *IEEE Trans. Mechatron.* **15** 448–59

Chen Z and Tan X 2010 Monolithic fabrication of ionic polymer–metal composite actuators capable of complex deformation *Sensors Actuators* A **157** 246–57

Curet O M, Patankar N A, Lauder G V and MacIver M A 2011a Aquatic manoeuvering with counter-propagating waves: a novel locomotive strategy *J. R. Soc. Interface* doi:10.1098/rsif.2010.0493

Curet O M, Patankar N A, Lauder G V and MacIver M A 2011b Mechanical properties of a bio-inspired robotic knifefish with an undulatory propulsor *Bioinsp. Biomimet.* **6** 026004

Donley J and Shadwick R 2003 Steady swimming muscle dynamics in the leopard shark *Triakis semifasciata J. Exp. Biol.* **206** 1117–26

Feinberg A W, Feigel A, Shevkoplyas S S, Sheehy S, Whitesides G M and Parker K K 2007 Muscular thin films for building actuators and powering devices *Science* **317** 1366–70

Flammang B E 2010 Functional morphology of the radialis muscle in shark tails *J. Morphol.* **271** 340–52

Geerlink P J 1989 Pectoral fin morphology: a simple relation with movement pattern? *Neth. J. Zool.* **39** 166–93

Geerlink P J and Videler J J 1987 The relation between structure and bending properties of teleost fin rays *Neth. J. Zool.* **37** 59–80

Geraudie J 1988 Fine structural peculiarities of the pectoral fin dermoskeleton of two Brachiopterygii, *Polypterus senegalus* and *Calamoichthys calabarisus* (Pisces, Osteichthyes) *Anat. Rec.* **221** 455–68

Geraudie J and Meunier F 1982 Comparative fine structure of the osteichthyan dermotrichia *Anat. Rec.* **202** 325–8

Goodrich E S 1904 On the dermal fin-rays of fishes, living and extinct *Q. J. Microsc. Sci.* **47** 465–522

Haas H J 1962 Studies on mechanisms of joint and bone formation in the skeletal rays of fish fins *Dev. Biol.* **5** 1–34

Hebrank M R 1982 Mechanical properties of fish backbones in lateral bending and in tension *J. Biomech.* **15** 85–9

Helfman G S, Collette B B and Facey D E 1997 *The Diversity of Fishes* (Malden, MA: Blackwell Science)

Jayne B C and Lauder G V 1994 Comparative morphology of the myomeres and axial skeleton in four genera of centrarchid fishes *J. Morphol.* **220** 185–205

Jayne B C and Lauder G V 1995a Are muscle fibers within fish myotomes activated synchronously? Patterns of recruitment within deep myomeric musculature during swimming in largemouth bass *J. Exp. Biol.* **198** 805–15

Jayne B C and Lauder G V 1995b Red muscle motor patterns during steady swimming in largemouth bass: effects of speed and correlations with axial kinematics *J. Exp. Biol.* **198** 1575–87

Jayne B C and Lauder G V 1996 New data on axial locomotion in fishes: how speed affects diversity of kinematics and motor patterns *Am. Zool.* **36** 642–55

Johnston I A 1981 Structure and function in fish muscle *Symp. of the Zoological Society of London* vol 84, pp 71–113

Johnston I A and Salamonski J 1984 Power output and force-velocity relationship of red and white muscle fibres from the pacific blue marlin (*Makaira nigricans*) *J. Exp. Biol.* **111** 171–7

Kato N 1999 Hydrodynamic characteristics of a mechanical pectoral fin *J. Fluids Eng.* **121** 605–13

Kato N 2000 Control performance in the horizontal plane of a fish robot with mechanical pectoral fins *IEEE J. Ocean. Eng.* **25** 121–9

Kim K and Tadokoro S (ed) 2007 *Electroactive Polymers for Robotic Applications* (Berlin: Springer)

Lanzing W J R 1976 The fine structure of fins and finrays of *Tilapia mossambica* (Peters) *Cell Tissue Res.* **173** 349–56

Lauder G V 2006 Locomotion *The Physiology of Fishes* 3rd edn, ed D H Evans and J B Claiborne (Boca Raton, FL: CRC Press) pp 3–46

Lauder G V, Anderson E J, Tangorra J and Madden P G 2007 Fish biorobotics: kinematics and hydrodynamics of self-propulsion *J. Exp. Biol.* **210** 2767–80

Lauder G V and Liem K F 1983 The evolution and interrelationships of the actinopterygian fishes *Bull. Mus. Comp. Zool. Harv.* **150** 95–197

Lauder G V and Madden P G A 2006 Learning from fish: kinematics and experimental hydrodynamics for roboticists *Int. J. Automat. Comput.* **4** 325–35

Lauder G V and Madden P G A 2007 Fish locomotion: kinematics and hydrodynamics of flexible foil-like fins *Exp. Fluids* **43** 641–53

Lauder G V, Madden P G A, Mittal R, Dong H and Bozkurttas M 2006 Locomotion with flexible propulsors I: experimental analysis of pectoral fin swimming in sunfish *Bioinsp. Biomimet.* **1** S25–34

Lauder G V and Tytell E D 2006 Hydrodynamics of undulatory propulsion *Fish Biomechanics* vol 23 *Fish Physiology* ed R E Shadwick and G V Lauder (San Diego, CA: Academic) pp 425–68

Long J H 1992 Stiffness and damping forces in the intervertebral joints of blue marlin (*Makaira nigricans*) *J. Exp. Biol.* **162** 131–55

Long J H, Hale M, McHenry M and Westneat M 1996 Functions of fish skin: flexural stiffness and steady swimming of longnose gar *Lepisosteus osseus J. Exp. Biol.* **199** 2139–51

Long J, Koob-Emunds M, Sinwell B and Koob T J 2002 The notochord of hagfish *Myxine glutinosa*: visco-elastic properties and mechanical functions during steady swimming *J. Exp. Biol.* **205** 3819–31

Long J H, Koob T J Jr, Irving K, Combie K, Engel V, Livingston N, Lammert A and Schumacher J 2006 Biomimetic evolutionary analysis: testing the adaptive value of vertebrate tail stiffness in autonomous swimming robots *J. Exp. Biol.* **209** 4732–46

Long J H and Nipper K S 1996 The importance of body stiffness in undulatory propulsion *Am. Zool.* **36** 678–94

Madden J, Vandesteef N A, Anquetil P, Madden P, Takshi A, Pytel R, Lafontaine S, Wieringa P A and Hunter I W 2004a Artificial muscle technology: physical principles and naval prospects *IEEE J. Ocean. Eng.* **29** 706–28

Madden P, Madden J, Anquetil P, Vandesteef N A and Hunter I W 2004b The relation of conducting polymer actuator material properties to performance *IEEE J. Ocean. Eng.* **29** 696–705

Marshall N B 1971 *Explorations in the Life of Fishes* (Cambridge, MA: Harvard University Press)

McHenry M J, Pell C A and Long J A 1995 Mechanical control of swimming speed: stiffness and axial wave form in undulating fish models *J. Exp. Biol.* **198** 2293–305

Mutlu R and Alici G 2010 Artificial muscles with adjustable stiffness *Smart Mater. Struct.* **19** 045004

Porter M E, Beltran J L, Koob T J and Summers A P 2006 Material properties and biochemical composition of mineralized vertebral cartilage in seven elasmobranch species (chondrichthyes) *J. Exp. Biol.* **209** 2920–8

Rome L, Loughna P T and Goldspink G 1984 Muscle fiber activity in carp as a function of swimming speed and muscle temperature *Am. J. Physiol.* **247** R272–9

Rome L C, Choi I, Lutz G and Sosnicki A 1992 The influence of temperature on muscle function in the fast-swimming scup. I. Shortening velocity and muscle recruitment during swimming *J. Exp. Biol.* **163** 259–79

Shadwick R E, Katz S L, Korsmeyer K E, Knower T and Covell J W 1999 Muscle dynamics in skipjack tuna: timing of red muscle shortening in relation to activation and body curvature during steady swimming *J. Exp. Biol.* **202** 2139–50

Shadwick R E and Lauder G V (ed) 2006 *Fish Biomechanics* vol 23 (San Diego, CA: Academic)

Shan Y, Philen M, Bakis C, Wang K and Rahn C 2006 Nonlinear-elastic finite axisymmetric deformation of flexible matrix composite membranes under internal pressure and axial force *Compos. Sci. Technol.* **66** 3053–63

Shinjo N and Swain G W 2004 Use of a shape memory alloy for the design of an oscillatory propulsion system *IEEE J. Ocean. Eng.* **29** 750–5

Standen E M and Lauder G V 2005 Dorsal and anal fin function in bluegill sunfish (*Lepomis macrochirus*): three-dimensional kinematics during propulsion and maneuvering *J. Exp. Biol.* **205** 2753–63

Standen E M and Lauder G V 2007 Hydrodynamic function of dorsal and anal fins in brook trout (*Salvelinus fontinalis*) *J. Exp. Biol.* **210** 325–39

Summers A and Long J 2006 Skin and bones, sinew and gristle: the mechanical behavior of fish skeletal tissues *Fish Biomechanics* vol 23 *Fish Physiology* ed R E Shadwick and G V Lauder (San Diego, CA: Academic) pp 141–77

Syme D A 2006 Functional properties of skeletal muscle *Fish Biomechanics* vol 23 *Fish Physiology* ed R E Shadwick and G V Lauder (San Diego, CA: Academic) pp 179–240

Taft N, Lauder G V and Madden P G 2008 Functional regionalization of the pectoral fin of the benthic longhorn sculpin during station holding and swimming *J. Zool. Lond.* **276** 159–67

Tangorra J, Anquetil P, Fofonoff T, Chen A, Del Zio M and Hunter I 2007a The application of conducting polymers to a biorobotic fin propulsor *Bioinsp. Biomimet.* **2** S6–17

Tangorra J L, Davidson S N, Hunter I W, Madden P G A, Lauder G V, Dong H, Bozkurttas M and Mittal R 2007b The development of a biologically inspired propulsor for unmanned underwater vehicles *IEEE J. Ocean. Eng.* **32** 533–50

Tangorra J L, Lauder G V, Hunter I, Mittal R, Madden P G and Bozkurttas M 2010 The effect of fin ray flexural rigidity on the propulsive forces generated by a biorobotic fish pectoral fin *J. Exp. Biol.* **213** 4043–54

Videler J J 1993 *Fish Swimming* (New York: Chapman and Hall)

Wang Z, Hang G, Wang Y, Li J and Du W 2008 Embedded sma wire actuated biomimetic fun: a module for biomimetic underwater propulsion *Smart Mater. Struct.* **17** 025039

Webb P W 1975 Hydrodynamics and energetics of fish propulsion *Bull. Fish Res. Board Can.* **190** 1–159

Webb P W 1978 Hydrodynamics: nonscombroid fish *Fish Physiology* vol VII *Locomotion* ed W S Hoar and D J Randall (New York: Academic) pp 189–237

Webb P W and Keyes R S 1982 Swimming kinematics of sharks *Fish. Bull.* **80** 803–12

Wiguna T, Heo S, Park H C and Goo N S 2009 Design and experimental parameteric study of a fish robot actuated by piezoelectric actuators *J. Intell. Mater. Syst. Struct.* **20** 751–7

Yeom S-W and Oh I-K 2009 A biomimetic jellyfish robot based on ionic polymer metal composite actuators *Smart Mater. Struct.* **18** 085002

Yim W, Lee J and Kim K J 2007 An artificial muscle actuator for biomimetic underwater propulsors *Bioinsp. Biomimet.* **2** S32–41

Young J Z 1981 *The Life of Vertebrates* (Oxford: Oxford University Press)

Zhang Z, Philen M and Neu W 2010 A biologically inspired artificial fish using flexible matrix composite actuators: analysis and experiment *Smart Mater. Struct.* **19** 094017